European benchmark on the ASTRID-like low-void-effect core characterization: neutronic parameters and safety coefficients

S. Borot, F. Alvarez-Velarde, E Fridman, I. Garcia Cruzado, N. Garcia Herranz, Diego Lopez, K. Mikityuk, A.-L. Panadero, S. Pelloni, A. Ponomarev, et al.

Proceedings of ICAPP 2015
May 03-06, 2015 - Nice (France)
Paper 15361

European benchmark on the ASTRID-like low-void-effect core characterization: neutronic parameters and safety coefficients

Sara Bortot[1], Francisco Alvarez-Velarde[2], Emil Fridman[3], Ignacio Garcia Cruzado[4], Nuria Garcia Herranz[4], D. López[2], Konstantin Mikityuk[1], Anne-Laurene Panadero[1], Sandro Pelloni[1], Alexander Ponomarev[5], Pierre Sciora[6], Armin Seubert[7], Haileyesus Tsige-Tamirat[8], Alfredo Vasile[6]

[1]*Paul Scherrer Institut (PSI), 5232 Villigen PSI, Switzerland*
[2]*Spanish National Research Centre for Energy, Environment and Technology (CIEMAT), Av. Complutense 40, 28040 Madrid, Spain*
[3]*Helmholtz-Zentrum Dresden-Rossendorf (HZDR), Bautzner Landstraße 400, 01328 Dresden, Germany*
[4]*Universidad Politécnica de Madrid (UPM), Jose Gutierrez Abascal 2, 28006 Madrid, Spain*
[5]*Karlsruhe Institute of Technology (KIT), Hermann-von-Helmholtz-Platz 1, 76344 Eggenstein-Leopoldshafen, Germany*
[6]*Commissariat à l´énergie atomique et aux énergies alternatives, CEA, DEN, DER/SPRC/LEDC, Cadarache, F-13108 Saint-Paul-lez-Durance, France*
[7]*Gesellschaft für Anlagen- und Reaktorsicherheit (GRS) mbH, Boltzmanntraße 14, 85748 Garching, Germany*
[8]*European Commission, Joint Research Centre, Institute for Energy and Transport (JRC), P.O. Box 2, NL-1755 ZG Petten, Netherlands*

Tel: +41 (0)56 310 4042, Fax: +41 (0)56 310 2327, Email:sara.bortot@psi.ch

Abstract – *A benchmark analysis was launched within the Work Package on Core Safety of the EU FP7 cross-cutting project supporting the European Sustainable Industrial Initiative (ESNII), named ESNII+, aimed at providing a quantitative estimation of the uncertainties affecting the re static neutronic parameters, including safety coefficients, of a Sodium-cooled Fast Reactor (SFR) low-void-effect core. The core is similar to the one considered for the Advanced Sodium Technological Reactor for Industrial Demonstration (ASTRID). Established deterministic and stochastic neutronic codes, as well as different nuclear data libraries, were employed by eight European organizations to perform a complete core characterization, with the ultimate goal to achieve consensus on computational methods and associated databases to be employed for advanced-design SFRs safety analyses. The comparison of the results obtained by the participating institutions provided quantitative information about capabilities and limitations of the different approaches, and about library effects, by highlighting the sensitivity of safety parameters to both computational techniques and nuclear data. Selected results of the first phase of the benchmark are presented and analyzed, along with a discussion of the planned R&D activities needed to improve the present benchmark status.*

I. INTRODUCTION

Significant efforts are currently devoted worldwide to boosting research and innovation on advanced fast reactor concepts, due to their great potential to improve the use of natural resources while reducing the amount of high-level radioactive waste, and to provide enhanced reliability and safety characteristics.

At a European level, a Task Force comprising research organizations and industrial partners was set to develop the European Sustainable Nuclear Industrial Initiative (ESNII), which addresses the need for demonstration of the prioritized Generation-IV fast reactor technologies; among the latter, the Sodium-cooled Fast Reactor (SFR) was selected as the reference solution.

In such a context, accurate modeling and assessment of SFR safety become essential to pursue this technology. Consequently, the capability to provide reliable predictions of the plant behavior under postulated accidental conditions is recognized as priority, making the verification of state-of-the-art computational tools and associated databases a first key step.

A number of benchmark exercises were set up and carried out aimed at validating, verifying and improving methodologies and computer codes used for the calculation of neutronic parameters and reactivity coefficients in SFRs.

Amongst others, it is worth recalling the Superphenix benchmark calculations, which were performed to compare core characteristics and to investigate the computational accuracy for the case of a large SFR core with high neutron leakage fraction[1]; the benchmark analyses for two BN-600 core design modifications carried out within the framework of the International Atomic Energy Agency (IAEA) sponsored Coordinated Research Project (CRP) on "Updated Codes and Methods to Reduce the Calculational Uncertainties of Liquid Metal-cooled Fast Reactors (LMFRs) Reactivity Effects"[2]; the benchmark analyses on the control rod withdrawal tests performed during the Phénix end-of-life experiments, sponsored and coordinated by the IAEA[3]; the benchmark exercise currently performed by the SFR Task Force (SFR-TF) constituted by the OECD/NEA within the Working Party on Reactor Systems (WPRS) with the objective of carrying out a comparative analysis of the safety characteristics of different fuels types for a large 3600MW_{th} U-Pu mixed oxide (MOX) SFR[4]; the DOE-CEA benchmark on the Advanced Sodium Technological Reactor for Industrial Demonstration (ASTRID) innovative core, which had the primary objective to assess key neutronics performance parameters and safety characteristics of the specified ASTRID configuration[5].

In the context of such a wide international effort for verification, validation and improvement of methods, codes and basic data currently employed in the field of fast reactor safety, a new benchmark exercise was launched as part of the contribution to the EU FP7 ESNII+ Project's Work Package on Core Safety, retaining the general objective to assess the viability and applicability of state-of-the-art tools and databases for ASTRID safety analyses. In fact, ASTRID features a medium-size (1500 MW_{th}), non-conventional, axially and radially heterogeneous core geometry entailing enhanced leakage characteristics, which are provided by the presence of a large sodium plenum zone atop the active core (present also in one of the BN-600 proposed design modifications) combined with an internal fertile zone within the inner fuel region[6]. Given such unique design features, accurate and reliable predictions of safety-relevant reactor physics parameters might result challenging. Therefore, a methodology assessment for the neutronics performance evaluation of a low sodium void worth core similar to the one considered for ASTRID[7] was performed upon commonly agreed calculation procedures. In particular, the general scope to identify capabilities and possible computational biases or limitations of existing methods, tools and basic data was pursued, along with the evaluation of the methodological uncertainties affecting the calculation of both core static neutronic parameters and safety coefficients to be employed for the subsequent safety analyses, with the ultimate goal to achieve consensus on computational methods.

Both deterministic and stochastic established neutronic codes, as well as different nuclear data libraries, were employed by eight European organizations (PSI, CEA, CIEMAT, GRS, HZDR, JRC, KIT and UPM) to perform a complete characterization of the core. The latter was modeled at End of Cycle (EoC) and operating conditions. Perturbations of the nominal state were applied according to guidelines directed to harmonizing the modeling approaches while ensuring that all relevant physical phenomena contributing to each reactivity coefficient are taken into account. Core multiplication factor, power peaking factors, kinetic parameters, reactivity feedback coefficients, coolant void and control system worth were calculated for the EoC reference configuration. The analysis was completed by including the study of nine coolant voiding scenarios, aimed at providing more detailed indications concerning the sodium void worth spatial dependence.

In this paper, selected results of this early phase of the benchmark and its major outcomes are presented and analyzed. In particular, a comparison of the first results obtained by the participating institutions is provided in order to convey initial, quantitative insights into (*i*) capabilities and advantages *vs.* limitations and weaknesses of different approaches (*e.g.*, deterministic *vs.* stochastic methods) and relative codes, and (*ii*) library effects: at this stage, the uncertainties introduced by the use of diverse tools, libraries and assumptions are evaluated, and the sensitivity of safety parameters to both nuclear data and computational techniques is highlighted, along with a discussion about future R&D activities planned to improve the present benchmark state-of-the-art. Broader-spectrum conclusions concerning the identification of the gaps in the current knowledge in the area of fast reactor core safety analysis are finally proposed.

II. BENCHMARK CORE CONFIGURATION

The ASTRID-like 1500 MW_{th} oxide-fueled core assumed as the reference for this study[7] presents a highly heterogeneous design: it features several driver zones combined with an inner fertile zone and a large sodium plenum above aimed at maximizing neutron leakage effects so as to achieve a negative overall coolant void worth (see Fig. 1).

As depicted in Fig. 2, the core is composed of 291 hexagonal wrapped fuel Sub-Assemblies (S/As) grouped into two radial regions, which differ for both plutonium content and axial zoning. The inner zone is composed of 177 S/As with a total active height of 1.1 m including a 0.2 m thick internal axial blanket; in order to reduce power peaking, the latter is not foreseen in the outer region, which counts 114 S/As with a total active height of 1.2 m. A 30 cm thick axial blanket is incorporated below both the inner and outer zone fissile fuel. Each S/A contains 217 pins in a triangular arrangement.

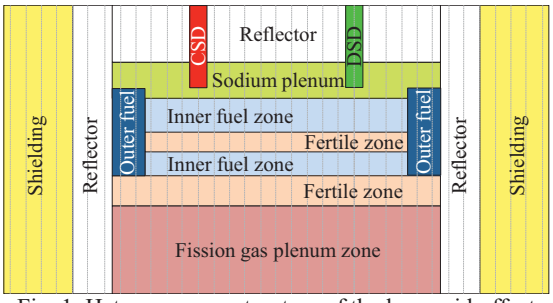

Fig. 1. Heterogeneous structure of the low-void-effect (ASTRID-like) core.

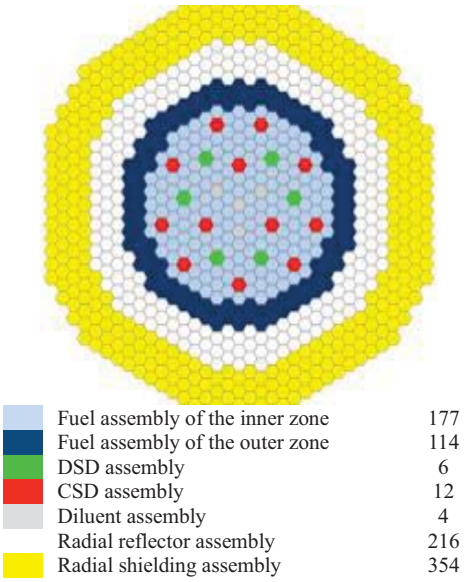

Fig. 2. ASTRID-like core map.

Regulation, compensation and safety functions are handled by 12 control rods (CSDs) and 6 safety rods (DSDs), respectively, all located within the inner core region, as well as 4 diluent assemblies. Three rings of radial reflector assemblies and four rows of radial shielding assemblies surround the active core.

Based on the design specifications at room temperature, a thermal expansion template was first developed so as to provide a unified set of geometrical parameters and material compositions at operating conditions (Table I). The resulting reactor global parameters at nominal power are summarized in Table II.

TABLE I

Core-average nominal temperatures at operating conditions.

Component	Temperature [°C]
Fuel (MOX @ EoC fissile/UO_2 @ EoC fertile)	1227/627
AIM1 cladding	475
Na coolant (average/inlet/outlet)	475/400/550
EM10 wrapper	475
316 Stainless steel diagrid	400

TABLE II

Main core global parameters at operating conditions.

Parameter	Value	Units
Nominal thermal power	1500	MW
Nominal mass flow rate	7752	kg s^{-1}
Number of S/As – inner core	177	-
Number of S/As – outer core	114	-
Number of CSDs (nat. and 48 % enr. B_4C)	12	-
Number of DSDs (48 % enr. B_4C)	6	-
S/A pitch	17.611	cm
Sodium inter-assembly gap thickness	0.473	cm
Inner fissile fuel height	60.456	cm
Outer fissile fuel height	90.685	cm
Internal axial blanket height	20.152	cm
Lower axial blanket height	30.228	cm
Sodium plenum height – inner core	39.555	cm
Sodium plenum height – outer core	29.479	cm

III. COMPUTATIONAL TOOLS AND DATABASES

The computational tools and nuclear data libraries chosen by each institution for the benchmark calculation of the ASTRID-like core safety parameters are listed in Table III.

TABLE III

Static neutronics computational tools and nuclear data libraries.

Institution	Codes	Libraries
KIT	KANEXT (Variant)	JEFF 3.1.1
PSI-E	ERANOS 2.2 (ECCO, Variant)	JEFF 3.1
CEA	ERANOS 2.3 (ECCO, Variant, BISTRO), PARIS	JEFF 3.1
GRS	HELIOS-1.12, FEM-DIFF-3D	HELIOS
PSI-S	Serpent 2	JEFF 3.1
HZDR-J	Serpent 2	JEFF 3.1
HZDR-N	Serpent 2	ENDF/B-VII.0
UPM	KENO-VI (SCALE6.2 beta)	ENDF/B-VII.0
CIEMAT	MCNP6.1	JEFF 3.1.1
JRC	MCNP5/MCNPX, MCNP6	JEFF 3.1

Concerning static neutronics, both deterministic and Monte Carlo codes were employed. The former include the European Reactor ANalysis Optimized calculation System (ERANOS)[8], the 3D discrete-ordinate solver PARIS[9], the KArlsruhe Neutronic EXtendable Tool (KANEXT)[10], Helios[11] and FEM-DIFF-3D[12]; the latter comprise Serpent[13], MCNP5, MCNPX and MCNP6[14], and the KENO-VI stochastic module of SCALE[15].

Regarding nuclear data, the majority of the calculations were performed using the European Joint Evaluated Fission and Fusion Files JEFF 3.1[16] and JEFF 3.1.1[17]; the US Evaluated Nuclear Data Library ENDF/B-VII.0[18] was employed in conjunction with both Serpent and SCALE, while an ENDF/B-VII-based library was used with HELIOS[11].

IV. BENCHMARK DEFINITION

The results for the following static neutronic performance and safety parameters are addressed in this paper:

- Core multiplication factor and kinetic parameters;
- Power distributions;
- CSD S-curve;
- Doppler constants;
- Coolant void worth.

It was recommended to model all core S/As heterogeneously, except for diluents, radial reflectors, and radial shielding assemblies, whose homogeneous description was provided, as well as for the upper section of inner and outer fuel S/As, occupied by the top shielding. In these latter cases, inter-assembly sodium gaps and steel wrappers were described heterogeneously, whereas the inner regions (*i.e.*, the regions inside the wrapper) were treated as homogeneous material mixtures whose volume fractions were provided.

Moreover, it the use of average, nominal operating temperatures for each material was recommended for cross-section calculations, except for control rods (CSDs) and safety rods (DSDs), which were decided to be kept at room temperature (i.e., lattice dimensions and compositions were assumed to be independent of core temperature variations).

The benchmark specifications and guidelines for the calculation of the selected parameters at nominal operating conditions and EoC are summarized hereinafter (it is noted that more reactivity feedbacks than presented in the paper were calculated and compared in the project, *e.g.* due to thermal expansion of diagrid, fuel/cladding, and coolant).

IV.A. Core Multiplication Factor and Kinetic Parameters

It was recommended to calculate core multiplication factor k_{eff} and kinetic parameters (*i.e.* effective delayed neutron fraction β_{eff}, and prompt neutron generation time Λ) with CSDs and DSDs in parking position.

IV.B. Power Distributions

As far as the axial peaking factors are concerned, it was required to provide one average value for each axial node, by employing a 5 cm mesh for the active core zones, and a single-node axial discretization for any non-fuel region.

As to the radial peaking factors, it was indicated to provide the power produced by each S/A normalized by the total power, following the numbering scheme in Fig. 3.

IV.C. CSD System Reactivity Worth

For the control system characterization, it was prescribed to calculate the respective S-curve by progressively inserting all the CSDs into the core by 10 % steps, the total insertion length corresponding to the distance between the top of the lower blanket region and the top of the outer core zone fuel rods (*i.e.* parking position). At hot conditions the total insertion length results 98.24 cm, and consequently each insertion step is equal to 9.82 cm.

IV.D. Doppler Constants

Four calculations were planned for the determination of the Doppler constant: two involving fissile fuel average temperature perturbations: namely, decrease from 1500 K to 1200 K (K_{D1}), and increase from 1500 K to 1800 K (K_{D2}), and two entailing fertile blanket average temperature perturbations: namely, decrease from 900 K to 600 K (K_{D3}), and increase from 900 K to 1200 K (K_{D4}).

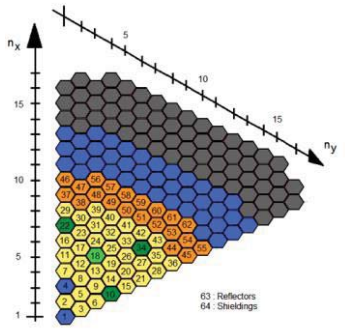

Fig. 3. 1/6 of core S/As and their associated numbering.

IV.E. Coolant Void Worth

The sodium void worth is defined by the reactivity change between the sodium voided and nominal states. In this benchmark, nine sodium voiding scenarios were specified (see Table V). A corresponding schematic representation of the regions to be voided is provided in Fig. 4.

TABLE V

Sodium voiding scenarios.

Case	Voided regions
S1	Everything above inner zone fissile (Above IF)
S2	Upper fissile region of inner zone only (Upper IF)
S3	Inner fertile region of inner zone only (IB)
S4	Lower fissile region of inner zone only (Lower IF)
S5	Everything above outer zone fissile (Above OF)
S6	Fissile region of outer zone only (OF)
S7	Everything above inner and outer zone fissile (Above IF + Above OF)
S8	Lower and upper fissile, and inner fertile region of inner zone; fissile region of outer zone (UIF + IB + LIF + OF)
S9	All fuel regions and all zones above, including inter-assembly gaps (UIF + IB + LIF + OF + AIF + AOF + IAG)

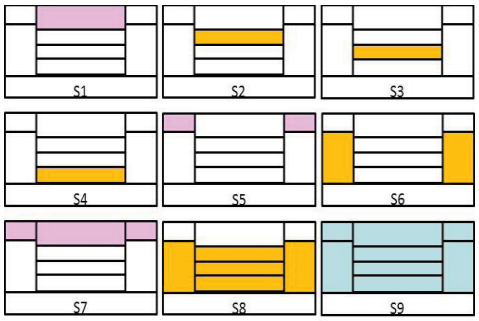

Fig. 4. Schematic representation of the core voiding scenarios: light violet indicates voiding of sodium plenum zones, amber—voiding of fuel zones and pale blue—total voiding, including inter-assembly gaps (IAG).

V. FIRST RESULTS

In this Section, a comparative collection of the results provided by each institution is presented and discussed.

V.A. Core Multiplication Factor and Kinetic Parameters

In Table VI the results for the core multiplication factor at EoC and nominal operating conditions (CSDs and DSDs in parking position) are summarized. It should be clarified that the discrepancy between two solutions using the ENDF/B-VII.0 data (HZDR-N and UPM) is partly explained by the fact that in the UPM solution 1200 K was set as the fissile temperature (instead of 1500 K), due to the unavailability of a temperature interpolation option in the calculational scheme used. Further discussions of the discrepancies in the multiplication factor calculations are deferred to Section V.C.

In Table VI the calculated effective delayed neutron fractions and prompt neutron generation times are presented as well. A good agreement is generally found among all the outcomes, as the different β_{eff} lie within a 20 pcm range. As far as the prompt generation time is concerned, the results exhibit a good agreement, the largest discrepancies being of the order of 10 %.

TABLE VI
Core multiplication factors and kinetic parameters.

Institution	k_{eff} [-]	β_{eff} [pcm]	Λ [10^{-7} s]
KIT	0.99966	358	4.54
PSI-E	1.00123	366	4.62
CEA	1.00432	356	4.55
GRS	1.00466	N/A	N/A
PSI-S	1.00431	347	4.72
HZDR-J	1.00394	357	4.73
HZDR-N	0.99796	344	4.76
UPM	1.00475	N/A	N/A
CIEMAT	1.00567	362	4.76
JRC	1.00218	350	4.82

V.B. Power Distributions

The results concerning the axial averaged power peaking factors are reported for the inner and outer fuel zones in Figs. 5a and 5b, respectively. All the results appear to be in a good agreement.

It is noted that accurate predictions of the flux gradient at the top of the core are vital for a correct estimation of the neutron leakage, and therefore for the calculation of the negative component of the void effect. Future analysis might include a comparison of the axial flux (or power) distribution in case of partial or total voiding of the sodium plenum above the core.

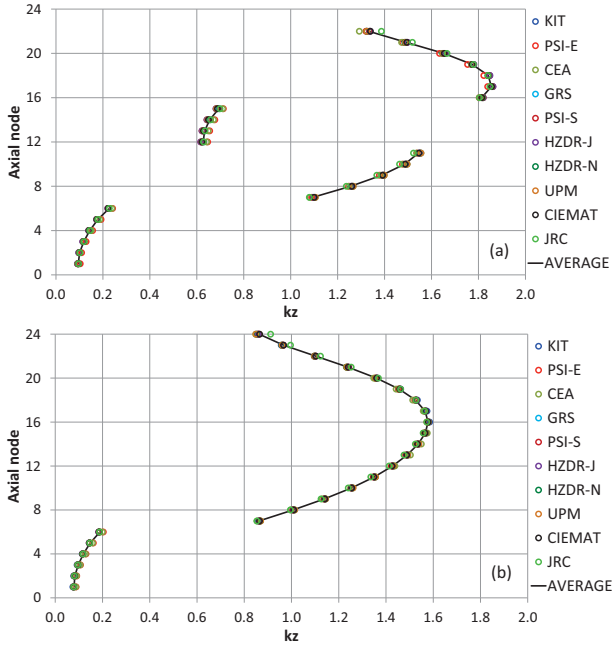

Fig. 5. Axial power peaking factors for the inner (a) and outer (b) core zones.

In Figs. 6a and 6b the assembly-wise mapping of power peaking factors is displayed for one sixth of the core and in particular for fuel and non-fuel S/As, respectively, as a function of their radial position. A satisfactory agreement among the partners is found for fuel subassemblies, while for the non-fuel regions only two codes (namely, ERANOS and MCNP6.1) can provide such results, and the discrepancy is too high (up to 100%), requiring further research and development particularly in the area of the gamma transport.

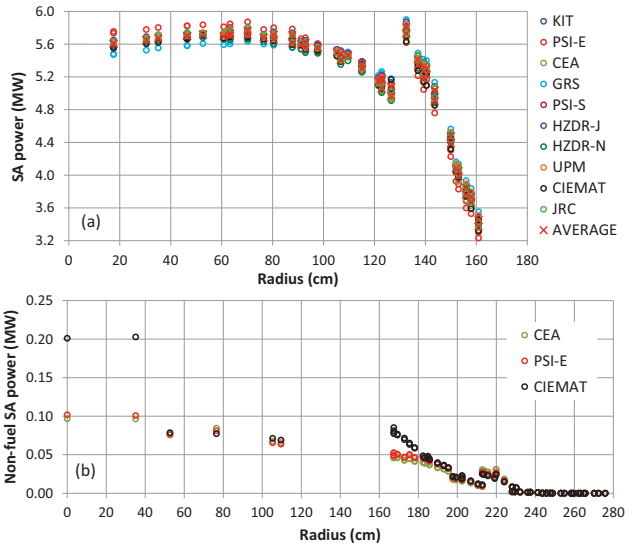

Fig. 6. Power for (a) fuel and (b) non-fuel S/As as a function of their radial position.

V.C. CSD System Reactivity Worth

In this section the results characterizing the CSD reactivity control system are presented.

The reactivity worth of CSDs was assessed as a function of the percentage of uniform insertion of the whole rod bank into the core (Fig. 7); in Fig. 8 the multiplication factor values for different positions of CSD rods (from parking position to 100 % inserted) are reported.

Regarding deterministic methods (first four solutions) in general, a quite good agreement among the different codes outcomes is observed. As far as the two ERANOS calculations are concerned, a systematic discrepancy of the order of 300 pcm between PSI and CEA results is found, the former giving higher values for the reactivity worth of CSDs. These effects are believed to be due to the method employed to generate absorber assemblies' group constants: PSI treated CSD and DSD cells by employing the current interface method using ECCO, whereas CEA evaluated the respective multi-group cross-sections by using an equivalence in reactivity method based on deterministic calculations qualified on stochastic and experimental cases.

Larger deviations from the average deterministic outcomes appear to affect KIT results, which increasingly underestimate k_{eff} along with the progressive insertion of the absorbers into the core.

Concerning Monte Carlo calculations performed by means of Serpent 2, a very good agreement is found between PSI and HZDR, whose results are consistent also with the deterministic outcomes discussed above. A quite significant role appears to be played by the nuclear data library, as the estimations accomplished by employing ENDF/B-VII.0 overestimate the absorbers worth by 600 pcm compared to JEFF 3.1 library. A similar discrepancy for k-effective between these libraries was found in another SFR-related benchmark[19].

Further studies are necessary to identify nuclides and reactions responsible for such large discrepancies.

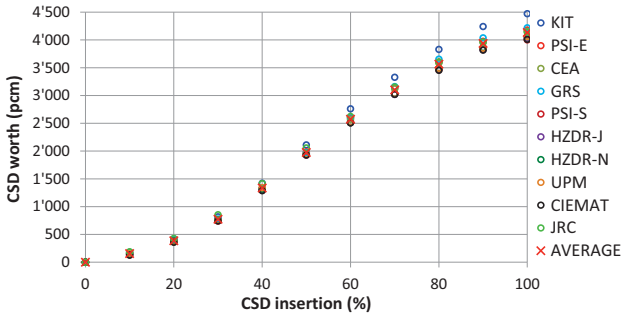

Fig. 7. Reactivity worth of all CSD rods (S-curve).

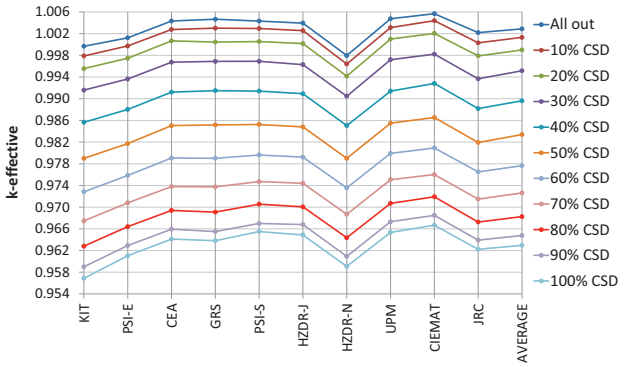

Fig. 8. Multiplication factor as a function of CSDs position.

V.D. Doppler Constants

In Table VII the fissile (K_{D1} and K_{D2}) and fertile (K_{D3} and K_{D4}) fuels' Doppler constants are reported. As a general remark, unexpectedly large discrepancies are found between the Doppler constant values obtained by applying two different temperature variations (*e.g.*, up to approximately 107 pcm for fissile fuel, and 80 pcm for fertile fuel), which only deterministic outcomes (fertile fuel case) are not affected by (largest discrepancy of the order of 9 pcm). Such differences appear to be more significant for stochastic codes, and therefore it can be argued that one possible cause might be a not sufficient statistics.

As far as the fissile fuel Doppler constant is concerned, the largest discrepancy among the different institutions' outcomes are of the order approximately 123 pcm for a 300 K temperature decrease, and of the order of 108 pcm for a 300 K temperature increase.

In the case of fertile fuel, the largest discrepancy among the different institutions' outcomes is of the order of 61 pcm for a 300 K temperature decrease, and of the order of 100 pcm for a 300 K temperature increase.

Further analyses are required to identify the causes for all the discrepancies.

TABLE VII

Doppler constants [pcm].

Institution	Fissile regions		Fertile regions	
	K_{D1}	K_{D2}	K_{D3}	K_{D4}
KIT	-623	-606	-314	-305
PSI-E	-684	-660	-321	-317
CEA	-661	-637	-327	-321
GRS	-576	-615	-278	-283
PSI-S	-661	-572	-335	-255
HZDR-J	-630	-594	-281	-311
HZDR-N	-583	-679	-285	-315
UPM	-584	-619	-273	-303
CIEMAT	-699	-592	-295	-234
JRC	-633	-612	-297	-333

IV.E. Coolant Void Worth

In Fig. 9 the coolant void worth results are collected for all the core voiding scenarios described in Section V. In addition, the results of the direct calculations involving the simultaneous voiding of more than one region are compared against the sum computed over each single zone worth in order to verify the additivity of the effect.

First of all, all solutions confirm that the total voiding of the studied core results in a negative reactivity effect (−400 pcm average). This total effect is a sum of a large positive effect from voiding of fuel regions (+1200 pcm average) and large negative effect from voiding of plenum regions (−1600 pcm average). This confirms that the goal of the low-void-effect core design aimed at enhancing the neutron leakage in case of sodium voiding is reached.

A reasonable agreement is generally found among the participants for all the scenarios foreseeing the voiding of active core regions. In particular, the spread of the void worth for inner fuel regions is below 100 pcm. When perturbing the outer fissile fuel, differences slightly rise compared with the inner core zone case, reaching a maximum value of 55 %. The void effects in the fuel regions are additive, as shown by the comparison between the curve "(Upper IF + IB + Lower IF + OF)" and the curve "(Upper IF) + (IB) + (Lower IF) + (OF)", differing by less than 3 %.

As far as the sodium plenum voiding is concerned, a larger discrepancy (up to 400 pcm) is observed especially for deterministic codes, reflecting the complexity of the neutron transport modeling in the voided regions above the fuel. The additivity of the void worth in the latter case is highlighted by the comparison between the curves "(Above IF) + (Above OF)" and "(Above IF + Above OF)", which result almost coincident.

The last scenario (# S9) under examination envisages the sodium voiding in all the regions perturbed in the previous cases, including the coolant inter-assembly gaps. Under such circumstances, larger discrepancies are found among the participants, especially as far as deterministic calculations are concerned (approximately 420 pcm spread). On the contrary, stochastic predictions seem to be in very good agreement, except for the case of JRC.

The two scenarios involving the full core voiding (red curves in Fig. 9) differ by approximately 200 pcm, which can be justified by the inter-assembly gap contribution, that was not included in any simulation except for scenario # S9 by any institution but KIT: in fact, the results provided by the latter ensue from voiding the inter-assembly gap in both cases, confirming the above-mentioned explanation.

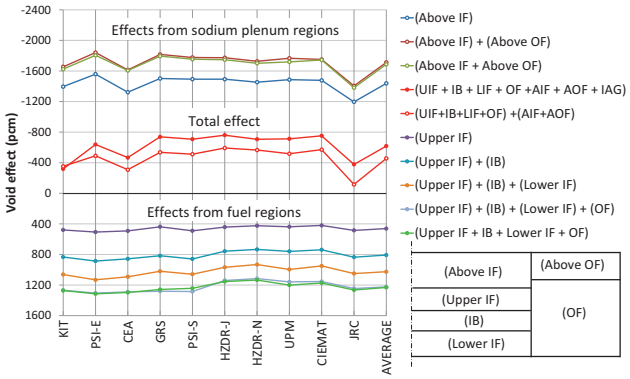

Fig. 9. Reactivity effects ensuing from voiding different regions of the core.

VI. CONCLUSIONS

A neutronic benchmark was launched in the frame of the FP7 EURATOM ESNII+ project with the participation of eight European institutions using ten codes and four nuclear data libraries, in order to study the main characteristics of a low-void-effect sodium-cooled fast spectrum core similar to the one of ASTRID at End-Of-Cycle conditions.

The studied core presents a number of non-conventional features (*e.g.* internal fertile zone between upper and lower fissile regions; fuel of different heights in inner and outer regions of the core) compared to the SFR core designs (*e.g.* Phénix, Superphenix, BN-600) for which neutronic codes and nuclear data libraries were benchmarked in the past.

In this respect, the present benchmark provided the unique opportunity to compare the performance of the current state-of-the-art neutronic codes for applications related to Generation-IV sodium-cooled fast reactor safety analyses.

The first results of this exercise are presented and briefly discussed in this paper.

As a major outcome of the study, the negative

reactivity effect ensuing from the total voiding of the core was unanimously confirmed.

Moreover, the code-to-code comparison allowed identifying a number of issues that require further clarifications and improvements. Some of them are mentioned here:

- The power generation in the non-fuel regions of the core was calculated by only two codes and the resulting results discrepancies reach 100 %. Further efforts are needed to improve the capability of the existing codes to predict the heat generation in SFR cores due to gamma transport.
- Unexpectedly large discrepancies (up to 100 pcm) were observed in the Doppler constants predictions. The reasons should be identified by additional simple calculations. The deviation of the Doppler effect's temperature dependence from a logarithmic law is also worth additional analysis.
- The discrepancy between nuclear data libraries (JEFF 3.1 and ENDF/B-VII.0), in particular for the prediction of CR worth, was observed in the current and also previous SFR-related benchmarks and therefore should be further clarified.
- The agreement between predictions of the void effect in the fuel regions is better than between estimations of the void effect in the sodium plenum regions. In the former zones the effect is mainly determined by the spectral hardening, while in the latter zones by the neutron leakage, which is evidently more difficult to model properly. Additional efforts are required to improve both the modeling of neutron transport in large voided volumes and (out of scope of this paper) the thermal-hydraulic simulation of the void evolution in the sodium plenum.

  In addition to the selected results presented in this paper, activities on the characterization of other reactivity effects (*e.g.* due to thermal expansions of diagrid, wrapper, fuel and cladding, as well as coolant temperature effects) are ongoing and will be reported later.

ACKNOWLEDGMENTS

The study has received funding from the European Community's Seventh Framework Programme (FP7/2007-2013) under the grant agreement n. 605172 (Euratom ESNII+) as well as under grant agreement n. 290605 (PSI-FELLOW/COFUND).

REFERENCES

1. J. TOMMASI *et al.*, "Benchmark on Superphenix calculations", *Proc. Int. Conf. on the Physics of Reactors (PHYSOR96)*, Mito, Ibaraki, Japan, September 16-20, 1996.

2. "BN-600 MOX Core Benchmark Analysis", IAEA-TECDOC-1700, International Atomic Energy Agency, Vienna, Austria, 2013.

3. "Benchmark Analyses on the Control Rod Withdrawal Tests Performed during the PHÉNIX End-of-Life Experiments", IAEA-TECDOC-1742, International Atomic Energy Agency, Vienna, Austria, 2014.

4. D. BLANCHET *et al.*, "AEN – WPRS Sodium Fast Reactor – Core Definitions, version 1.2", September 19th 2012. https://www.oecd-nea.org/science/wprs/sfr-taskforce/WPRS-AEN-SFR-Cores-V1.2.pdf

5. J. BESS *et al.*, "DOE-CEA Benchmark on SFR ASTRID Innovative Core: Neutronic and Safety Transients Simulation", *Proc. Int. Conf. Fast Reactors and Related Fuel Cycles: Safe Technologies and Sustainable Scenarios (FR13, IAEACN-199/281)*, Paris, France, March 4-7 (2013).

6. P. SCIORA *et al.*, "Low void effect core design applied on 2400 MWth SFR reactor", *Proc. of ICAPP 2011*, Nice, France, May 2-5, 2011.

7. F. VARAINE *et al.*, "Pre-conceptual design study of ASTRID core", *Proc. of ICAPP 2012*, Chicago, USA, June 24-28, 2012.

8. G. RIMPAULT *et al.*, 2002. "The ERANOS data and code system for fast reactor neutronic analyses", *Proc. Int. Conf. on the New Frontier of Nuclear Technology: Reactor Physics, Safety and High-Performance Computing (PHYSOR 2002)*, Seoul, Korea, October 7-10.

9. R. LE TELLIER *et al.*, "High-order discrete ordinate transport in hexagonal geometry: a new capability in ERANOS", *Il Nuovo Cimento*, **33 C**, 1, 121 (2010).

10. S. VAN CRIEKINGEN *et al.*, "The KANEXT modular program for reactor physics calculations", INR Seminar, May 28 2009, http://cornelis-broeders.homelinux.net/pdfs/KANEXTseminar_INR_2009.pdf

11. J.J. CASAL *et al.*, "HELIOS: Geometric Capabilities of a New Fuel-Assembly Program", *Proc. Int. Top. Mtg. Adv. Math. Comp. Reac. Phys.*, Pittsburg, PA, USA, **Vol. II**, Sect. 10.2.1, 1-13 (1992).

12. A. SEUBERT, "3-D few-group unstructured geometry finite element diffusion solver", GRS development.

13. J. LEPPANEN, "Serpent – a Continuous-energy Monte Carlo Reactor Physics Burnup Calculation Code", User's Manual, March 2013, http://montecarlo.vtt.fi/download/Serpent_manual.pdf

14. "A General Monte Carlo N-Particle (MCNP) Transport Code", Los Alamos National Laboratory, https://mcnp.lanl.gov/

15. SCALE: A Comprehensive Modeling and Simulation Suite for Nuclear Safety Analysis and Design, ORNL/TM-2005/39, Version 6.1. http://scale.ornl.gov/publications.shtml

16. A. KONING *et al.*, "The JEFF-3.1 Nuclear Data Library", *JEFF Report 21* (2006).

17. A. SANTAMARINA *et al.*, "The JEFF-3.1.1 Nuclear Data Library", *JEFF Report 22, Validation Results from JEF-2.2 to JEFF-3.1.1* (2009).

18. M.B. CHADWICK *et al.*, "ENDF/B-VII.0: Next Generation Evaluated Nuclear Data Library for Nuclear Science and Technology", *Nuclear Data Sheets*, **107**, 12, 2931-3060 (2006).

19. L. BUIRON *et al.*, "Evaluation of large 3600MWth sodium-cooled fast reactor OECD neutronic benchmarks", PHYSOR 2014 – The Role of Reactor Physics Toward a Sustainable Future, The Westin Miyako, Kyoto, Japan, September 28 – October 3, 2014.